



# Fingerprint Quality Assessment Combining Blind Image Quality, Texture and Minutiae Features

Z Yao, Jean-Marie Le Bars, Christophe Charrier, Christophe Rosenberger

► **To cite this version:**

Z Yao, Jean-Marie Le Bars, Christophe Charrier, Christophe Rosenberger. Fingerprint Quality Assessment Combining Blind Image Quality, Texture and Minutiae Features. ICISSP 2015, Feb 2015, <http://www.icissp.org/Home.aspx>, France. <hal-01097723>

**HAL Id: hal-01097723**

**<https://hal.archives-ouvertes.fr/hal-01097723>**

Submitted on 21 Dec 2014

**HAL** is a multi-disciplinary open access archive for the deposit and dissemination of scientific research documents, whether they are published or not. The documents may come from teaching and research institutions in France or abroad, or from public or private research centers.

L'archive ouverte pluridisciplinaire **HAL**, est destinée au dépôt et à la diffusion de documents scientifiques de niveau recherche, publiés ou non, émanant des établissements d'enseignement et de recherche français ou étrangers, des laboratoires publics ou privés.

# Fingerprint Quality Assessment Combining Blind Image Quality, Texture and Minutiae Features

Z. Yao, J. Le bars, C. Charrier and C. Rosenberger

*Universite de Caen Basse Normandie; ENSICAEN; UMR 6072 GREYC, Caen, France.*

{*jean-marie.lebars; christophe.charrier*}@unicaen.fr {*zhigang.yao; christophe.rosenberger*}@ensicaen.fr

Keywords: Fingerprint, minutiae template, quality assessment, evaluation.

Abstract: Biometric sample quality assessment approaches are generally designed in terms of utility property due to the potential difference between human perception of quality and the biometric quality requirements for a recognition system. This study proposes a utility based quality assessment method of fingerprints by considering several complementary aspects: 1) Image quality assessment without any reference which is consistent with human conception of inspecting quality, 2) Textural features related to the fingerprint image and 3) minutiae features which correspond to the most used information for matching. The proposed quality metric is obtained by a linear combination of these features and is validated with a reference metric using different approaches. Experiments performed on several trial databases show the benefit of the proposed fingerprint quality metric.

## 1 INTRODUCTION

Fingerprint systems, among biometric modalities, are the most deployed solution due to the invariability, usability and user acceptance of fingerprints (Jain et al., 2004). So far, the application of fingerprint is no longer limited to traditional public security area (official applications), but spread into the daily life, smart phone authentication and e-payment, for instance. Because of the continuous developments, fingerprint quality assessment has become a crucial task in the deployment of systems in real applications. There is no doubt that a good quality sample during the enrollment process can reduce recognition errors. The good quality of a fingerprint sample is also beneficial to matching operations (Grother and Tabassi, 2007) in addition to the clarity of human intuition and feature extractability of the image (Chen et al., 2005). In this case, most previously proposed fingerprint quality approaches have been implemented in terms of utility of biometric sample's quality rather than fidelity (Alonso-Fernandez et al., 2007), i.e. biometric sample's quality should be related to system performance. Tabassi *et al.* (Tabassi et al., 2004) defined their quality metric as a predictor of system performance by considering the separation of genuine matching scores (GMS) and impostor matching scores (IMS). Chen *et al.* (Chen et al., 2005) later proposed one quality metric by considering authentication performance.

As we can see in the literature, features are very important to make a reliable judgment of the quality of a fingerprint. Moreover, a fingerprint can be considered as an image or a set of minutiae we could extract many features. This study proposes a quality metric of fingerprint image based on the utility property by considering two aspects in general: 1) the fingerprint image itself and 2) the corresponding minutiae template which is rarely taken into account for this issue. The validation of the proposed quality metric is carried out by using two approaches based on the prediction of authentication performance. The main contribution of the paper is to propose a continuous quality index of a fingerprint integrating different points of view (brought by the used features) and providing a better assessment.

This paper is organized as follows: Section 2 details the features for computing the proposed quality metric. Section 3 presents the computation approach of the proposed quality metric. Experimental results are given in 4. Conclusion is given in section 5.

## 2 QUALITY FEATURES

The general purpose of this work is to qualify original fingerprint samples and to analyze the proposed quality metric through different validation ap-

proaches. The proposed quality metric is based on a former method in (El Abed et al., 2013). That work evaluated altered fingerprint image quality with two kinds of quality features, one is universal (no reference image quality assessment) and another is related to the fingerprint modality. We employ this framework for the original fingerprint samples.

## 2.1 NR-IQA and Prior Features

In (El Abed et al., 2013), 11 features have been used to obtain the quality metric, including one derived from a NR-IQA algorithm (Saad et al., 2012) and the others are image-based features. Details of the feature are not presented again in this paper. A general description is given in table 1.

Table 1: List of quality features in (El Abed et al., 2013)

Feature	Description	NO.
NR-IQA	BLIINDS (Saad et al., 2012)	1-N1
SIFT point number	Number of SIFT keypoints	2-S1
SIFT DC coefficient	DC coefficient of SIFT features	3-S2
SIFT Mean	Mean measure related to SIFT keypoints	4-S3
SIFT STD	Standard deviation related to SIFT keypoints	5-S4
Block number	Number of blocks ( $17 \times 17$ )	6-P1
Patch RMS Mean	Mean of blocks RMS <sup>1</sup> values.	7-P2
Patch RMS STD	Standard deviation of RMSs	8-P3
Patch RMS Median	Median of blocks RMSs.	9-P4
Patch RMS skewness	Skewness of blocks RMSs.	10-P5
Median LBP	256-level MBP histogram	11-P6

1. 'RMS' is the abbreviation of Root Mean Square.

Salient features are extracted by using Scale Invariant Feature Transform (SIFT) operator. For patched features, it firstly divide images into blocks of  $17 \times 17$ , and then the root mean square (RMS) value of each block is computed to obtain the quality features.

## 2.2 Texture-based Quality Features

Texture features are widely used for image classification and retrieval applications. There is not study observed that whether some of them are able to contribute distinctive results for quality assessment of fingerprint image. In this study, 11 texture features have been selected as the components for generating the proposed quality metric, cf. 2. These features have been classified into four classes:

- 1) The first class of textural features embeds local binary pattern (LBP) features and its extensions or transforms. LBP features have been proposed by Ojala et al (Ojala et al., 2002) for image classification. This feature is simple yet efficient so that it is widely used for texture analysis. The idea of LBP operator was that the two-dimensional surface textures can be described by two complementary measures: local spatial pattern and gray scale contrast (Pietikäinen, 2011). Basic LBP operator generates a binary string by thresholding each 3-by-3 neighborhood of every pixel of the image.

Table 2: List of texture features.

Feature	Format	NO.
LBP	256-level LBP histogram vector	1-C1
Four-patch LBP	Descriptor code vector	2-C1
Completed LBP	512-bit 3D joint histogram vector	3-C1
GLCM measures	8-bit GLCM vector	4-C2
LBP H-FT	LBP histogram FT <sup>1</sup> vector	5-C1
2S 16O <sup>1</sup> Gabor	64-bit Gabor response vector	6-C3
4S 16O Gabor	128-bit Gabor response vector	7-C3
8S 16O Gabor	256-bit Gabor response vector	8-C3
16S 16O Gabor	512-bit Gabor response vector	9-C3
LRS	81-bit LRS motif histogram vector	10-C4
Median LBP	256-level MBP histogram	11-C1

1. 'S', 'O' and 'FT': abbr. of scale, orientation and Fourier Transform.

The transforms of LBP involved in this study include four-patch LBP (FLBP), completed LBP (CLBP), LBP histogram Fourier transform (LBPHFT) (Nanni et al., 2012) and median LBP (MLBP) (Hafiane et al., 2007).

- 2) Second class is Haralick feature or gray level co-occurrence matrix (GLCM) (Haralick et al., 1973). In this study, 4 statistic measures generated from the GLCM matrix in 4 directions combination of neighbor pixels are computed, including energy, entropy, moment and correlation.
- 3) The 2D Gabor decomposition is a sinusoidal function modulated by a Gaussian window. In this case, the basis of a Gabor function is complete but not orthogonal. In the last few decades, it has been widely applied to fingerprint image and other biometric data to perform classification and segmentation tasks. Shen *et al.* (Shen et al., 2001) proposed using Gabor response to evaluate fingerprint image quality, in which it is said that one or several Gabor features of 8-direction Gabor response are larger than that of the others. Olsen *et*

*al.* (Olsen et al., 2012) proposed a quality index based on 4-direction Gabor response and it is said that 4-direction is sufficient to qualify fingerprint. However, in this study, it is observed that 2-scale 4-direction Gabor filters do not bring out distinctive regularity for fingerprint images of a specified database.

- 4) The last one concerns local relational string (LRS) (Hafiane and Zavidovique, 2006) which is an illumination invariant operator and it reflects variation of local gray level of the image. The operator is based on the local pixels relation in a specified scale, and it uses 3 relations to generate local relation motif histogram for measuring local spatial variations of the image.

### 2.3 Minutiae-based Quality Features

Feng *et al.* (Feng and Jain, 2011) proposed to reconstruct a fingerprint image from the triplet representation of minutia point. Such a result demonstrates the significance of minutiae template. In this study, we relate the minutiae template to the quality assessment of fingerprint by defining several quality features based on minutiae number and DFT of the three components of minutiae point, as shown in table 3.

Table 3: Minutiae number-based measures related to fingerprint quality.

Measure	Description	NO.
Minutiae number (MN)	Minutiae number of fingerprint.	1-M1
Mean of minutiae DFT	Defined as equation (1b)	2-M1
STD of minutiae DFT	Equation (1c)	3-M1
MN in ROI <sup>1</sup>	MN in a rectangle region.	4-M1
MN in ROI 2	MN in a circle region.	5-M1
Region-based RMS	Root mean square (RMS) value of MN based on two blocks of the template.	6-M1
Region-based median	Median value of MN obtained by dividing the template into 4 blocks.	7-M1
Block-based measure	A block-based score for the template.	14-M1

1. region of interest.

Minutiae-based measures given in table 3 are calculated based on a the template of detected minutiae extracted by using NBIS tool (Watson et al., 2007). This template contains a quadruple representation of minutia point which consists of 1) the position  $(x,y)$  of detected minutiae, 2) the

orientation  $\theta$  of detected minutiae, and 3) a quality score of detected minutiae. In the experiment, only the minutiae positions and orientations are used for calculating these measures. In the following, the details of some of the measures are presented.

In the experiment, both measure 2 and 3 are derived from the magnitude of the Fourier transform of the linear combination of 3 minutia components after eliminating DC component, as described in equation 1.

$$F(x, y, \theta) = \sum_{n=0}^{N-1} x_n \cdot \mu^{kn} + y_n \cdot \nu^{kn} + \theta \cdot \omega^{kn}. \quad (1a)$$

where  $\mu$ ,  $\nu$ , and  $\omega$  are frequency samples. Measures  $M_2$  and  $M_3$  are finally computed as follows:

$$M_2 = \overline{|F(x, y, \theta)|}, \quad (1b)$$

$$M_3 = \sqrt{\frac{1}{N} \sum_{i=1}^N (F_i - M_2)}. \quad (1c)$$

DC component was eliminated when computing these two measures because there is no valuable information in this element.

For measure 4, the size of rectangle region is determined by the maximum value of both  $x$  and  $y$  coordinates of minutiae, for which there is no useful information outside the foreground of the fingerprint in this case. This choice also ensures that the region of interest will not go over the effective area of minutiae. An example of rectangle region is shown in figure 1 (a).

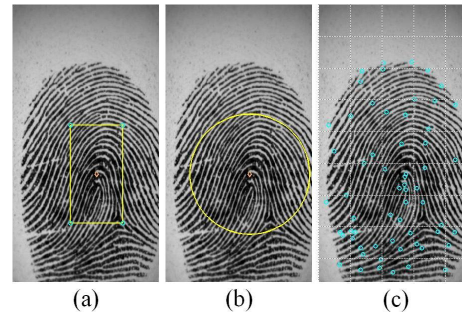


Figure 1: Example of circle region (a), rectangle region (b), and template block partition in the size of fingerprint (c).

The radius of the circle region for measure 5 is also determined by the maximum and minimum location value of minutiae along the horizontal direction of fingerprint, for minutiae lie around fingerprint center are said to be those who contribute most to fingerprint matching, i.e. they are considered as the most informative. As the quadruple representation does not provide information of fingerprint core

point, an estimated point was used as the center’s location of the fingerprint. A comparison has been made between the estimated center point and a core point detected by another approach, and it is found that the result does not vary too much. The estimated center position was determined by considering the maximum and minimum minutiae location as well. An example of the circular region is shown in figure 1 (b).

For measures 6 and 7, the whole fingerprint region is divided into 2 and 4 blocks, and minutiae number in each block is considered to generate a measure. Another block-based measure is calculated by dividing the whole fingerprint region into several blocks in the size of  $64 \times 64$ . The blocks are classified into 3 classes, reasonable block, vague block, and unreasonable block. At last, a quality index is assigned to each block in terms of the minutiae number in the block, for which a threshold is used for determining the index of each block. An example of block partition is shown by figure 1 (c). In addition, features proposed in (Ross et al., 2005) are calculated in terms of minutiae distribution and orientations, and they are rotation and translation invariant.

We analyse in section 4.2 the behavior of these quality features. Based on all these quality features, we generate a quality metric using the method described in the next section.

### 3 QUALITY METRIC DEFINITION

The quality metric of fingerprint (QMF) image in this study is computed by an approach using a Genetic Algorithm (GA) proposed in (El Abed et al., 2013). It uses a weighted linear combination of the quality features, formulated as

$$Q = \sum_{i=1}^N \alpha_i F_i, \quad (2)$$

where  $N$  is the number of quality features  $F_i$  ( $i = 1, \dots, N$ ),  $\alpha_i$  are the weighted coefficients. The weighted coefficients are computed via optimizing a fitness function of GA which is composed by the Pearson correlation between combined quality results defined by equation 2 and corresponding GMS of fingerprints samples. This approach realizes a learning of quality assessment and optimizes the weighted coefficients to generate a continuous quality metric combining different features.

## 4 EXPERIMENTAL RESULTS

In order to validate the behavior of the quality metric (denoted as QMF) of this study, an analysis of the proposed features is realized. The validation of QMF is implemented by observing the evaluation results of both QMF and NFIQ (Tabassi et al., 2004).

### 4.1 Protocol and Databases

In this study, three FVC databases (Maio et al., 2004) have been used for experiments: FVC2002DB2A, FVC2004DB1A, and FVC2004DB3A. The first two databases are established by optical sensor and the last one is thermal sweeping sensor. The resolutions and image dimensions of all 3 databases are 500dpi, 500dpi, 512dpi, and  $296 \times 560$ ,  $480 \times 640$ , and  $300 \times 480$ , respectively. Each database involves 100 fingertips, and 8 samples for each fingertip. The intra-class and inter-class matching scores involved in the experiment have been calculated by using NBIS tool (Watson et al., 2007) namely Bozorth3 and a commercial SDK (IDt, ). Minutiae template used in the experiment were also extracted by using the corresponding MINDTCT and the SDK. The minutiae-based features involve in only the location  $(x, y)$  and the orientation  $\theta$  of minutia so that we don’t consider the quality value of the points (generated by MINDTCT) and the type of them (given by SDK).

### 4.2 Feature Analysis

Fernandez *et al.* (Alonso-Fernandez et al., 2007) and Olsen (Olsen et al., 2012) respectively calculated Pearson and Spearman correlation coefficients between different quality metrics to observe the behaviour of them. We use the same approach in this study by computing the Pearson correlation between several quality metrics and the QMF. Quality metrics used for this analysis include OCL (Lim et al., 2002), orientation flow (OF) (Chen et al., 2004), standard deviation (STD) (Lee et al., 2005), Pet Hat’s wavelet (PHCWT) (Nanni and Lumini, 2007) and NFIQ. Figure 5, 7, 6 presents the correlation results obtained from the trial databases for all quality features.

In table 5, highlighted columns (with yellow) demonstrated a relatively stable correlation for all the three databases, and some others marked with green illustrated their feasibility for certain data sets. According to this observation, we could make an attempt to reduce some redundant features in next study. Table 7 presents only 11 of the minutiae-based features, for the correlation of them is not very dis-

tinctive. Some of them demonstrate good correlated behavior with the quality metrics, but greatly vary among the data sets and even not correlated with any of the quality metrics. Likewise, the correlation results of the image-based features are given in table 6. We use all these features to calculate the quality metric which enables qualifying fingerprint samples with complementary information. Note that the last columns denote relatively good correlation between the NR-IQA and the quality metrics.

### 4.3 Metric validation

The validation involves in two sections, one is the impact of enrollment selection (YAO et al., 2014) and another is a utility evaluation (Chen et al., 2005).

#### 4.3.1 Impact on the enrollment process

Authors in (Grother and Tabassi, 2007) discussed on quality values used for three different cases, including enrollment phase, verification task and identification. Enrollment is generally a supervised task for getting relatively good quality samples, and one main difference between verification and identification tasks is the existence of enrollment which directly impacts on how FNMR and FMR acts. However, if the purpose is to validate a quality metric without considering the testing type (i.e. algorithm testing, scenario testing and etc.), the variation of enrollment samples quality would generate distinctive impacts on matching performance and the result is repeatable in the experiments.

We computed the EER values of 3 databases by choosing the best quality samples as the reference (by using NFIQ and QMF). A good quality metric for the choice of the references should reduce matching error rate. The ROC curves and EER values of FVC2004DB1A based on this strategy are presented as an illustration, see figure 2.

The EER values by using NFIQ (for the enrollment process) is 14.8%, and 14.1% with the QMF metric. For FVC2002DB2A and FVC2004DB3A, the EER values are 13.2% (NFIQ), 10.6% (QMF), 8.3% (NFIQ) and 6.7% (QMF). These results show the benefit of QMF face to NFIQ as it permits to optimize the enrollment process.

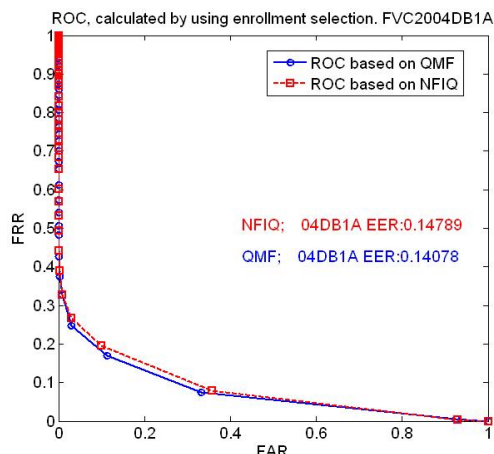


Figure 2: Enrollment selection result of FVC2004DB1A.

In addition, such EER values are calculated via the commercial SDK, results obtained via NFIQ are 3.99% (02DB2A), 9.39% (04DB1A) and 4.76% (04DB3A), while the values obtained by using QMF are 3.39% (02DB2A), 5.35% (04DB1A) and 4.64% (04DB3A), respectively. This result demonstrates whether the QMF is possible for dealing with interoperability. However, in practical, this property relies on both the performance of matching algorithm and the quality metric. We employ this result simply for validating the QMF.

#### 4.3.2 Quality and performance evaluation

The second approach is based on the isometric bins of samples sorted in an ascending order the quality values and is more strict for the distribution of the quality values. In order to validate the QMF by referring to NFIQ, instead of dividing quality values of NFIQ into 5 isometrics bins, we divided them into 5 bins which correspond to its 5 quality labels. The reason for doing so is that NFIQ fails to satisfy the isometric-bin evaluation criteria, as given in figure 3.

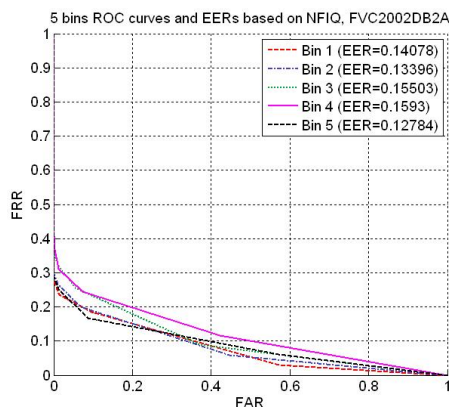


Figure 3: Example of 5-bin evaluation for NFIQ on FVC2002DB2A.

Then, the EER values of the divided bins are calculated. For NFIQ-based quality values, it is easier to calculate the EER values of the 5 label bins, as it is depicted in figure 4.

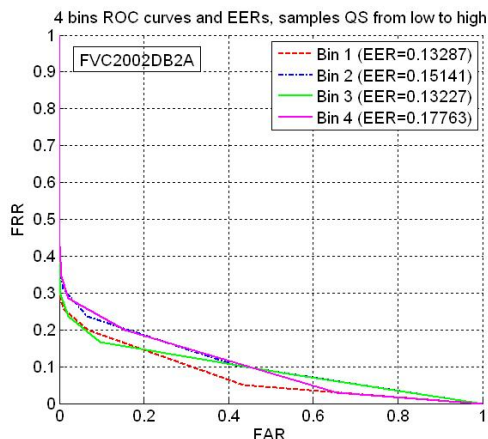


Figure 4: Monotonic increasing matching performance validation of FVC2002DB2A for NFIQ, calculated by dividing quality values into 5 isometric bins (no sample of quality 5 for this database).

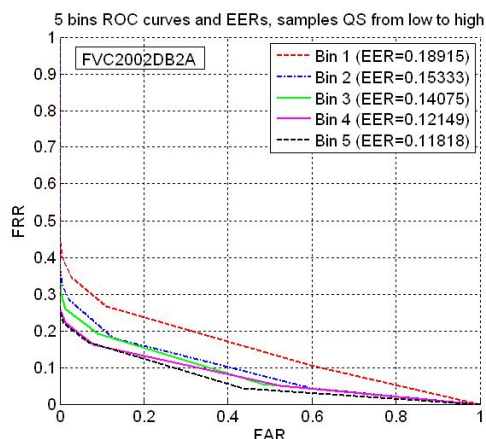


Figure 5: Monotonic increasing matching performance validation of FVC2002DB2A for QMF, calculated by dividing quality values into 5 isometric bins.

We are able to observe that the matching performances on FVC2002DB2A and FVC2004DB3A are monotonically increased by pruning bad quality samples gradually. NFIQ generated quality levels from 1 to 4 for FVC2002DB2A, and no samples of level 5 were figured out for this database. This might be due to the minutiae points detected on the images of this database, because NFIQ algorithm involves in minutia quality of the fingerprint image. This situation was observed when calculated the correlation between 14 minutiae quality features and genuine matching scores in the experiment of this study. It shows a relatively higher correlation on FVC2002DB2A,

while the values of two other databases are relatively lower. For FVC2004DB1, both the proposed quality metric and the reference algorithm showed certain difficulties. Here, only the graphical results on FVC2002DB2A are presented, while the 5 bins' EER values based on proposed approach and NFIQ of FVC2004DB1A and FVC2004DB3A are given in table 4. The quality values of QMF are normalized into [0, 100] on each database where small value denotes bad quality (bin 1). The NFIQ has 5 quality levels where level 1 represents the best quality and level 5 is the worst one.

Table 4: 5 bins EER values based on QMF and NFIQ of FVC2004DB1A and FVC2004DB3A.

Bin No.	B1	B2	B3	B4	B5
Q <sup>1</sup> . (04DB1)	22.2%	16.6%	17.2%	17.8%	13.3%
N <sup>1</sup> . (04DB1)	15.8%	18.1%	17.7%	23.2%	26.5%
Q. (04DB3)	14.2%	8.9%	7.4%	5.8%	4.2%
N. (04DB3)	7.5%	8.1%	13.4%	12.9%	29.8%

1. 'Q' and 'N' are abbreviation of 'QMF' and 'NFIQ', respectively.

## 5 CONCLUSION

This study first propose a fingerprint quality metric by considering image-based quality features and those derived from minutiae template. Second, the quality metric has been validated by using different validation approaches. In the study, the proposed quality metric was evaluated on 3 different FVC databases, FVC2002 DB2 A, FVC2004 DB1 A, and FVC2004 DB3 A. Among the validation result, it can be observed that the performance of quality metric shows a great variation between different databases, where both the reference quality algorithm and proposed quality metric obtain relatively good result on FVC 2004 DB3 A. This is due to several factors impacted on image quality and matching performance. In addition to external factors such as sensor type (Ross and Jain, 2004) and environment, it might be involved in image factors, such as contrast, image size, pixel density, foreground and background area; and correspondingly the factors caused by minutiae template, such as minutiae location, minutiae reliability, and other minutiae properties if they are considered.

In this study, a lot of quality features were adopted for generating quality metric. In this case, it is necessary to analyze the redundancy of quality feature in the future work. Besides, in order to improve the current quality metric, future works of this study will also focus on feature processing for the quality metric.

## REFERENCES

- User friendly toolkit for easy integration of state of the art fingerprint recognition technology.
- Alonso-Fernandez, F., Fierrez, J., Ortega-Garcia, J., Gonzalez-Rodriguez, J., Fronthaler, H., Kollreider, K., and Bigun, J. (2007). A comparative study of fingerprint image-quality estimation methods. *Information Forensics and Security, IEEE Transactions on*, 2(4):734–743.
- Chen, T., Jiang, X., and Yau, W. (2004). Fingerprint image quality analysis. In *Image Processing, 2004. IICIP '04. 2004 International Conference on*, volume 2, pages 1253–1256 Vol.2.
- Chen, Y., Dass, S. C., and Jain, A. K. (2005). Fingerprint quality indices for predicting authentication performance. In *Audio-and Video-Based Biometric Person Authentication*, pages 160–170. Springer.
- El Abed, M., Ninassi, A., Charrier, C., and Rosenberger, C. (2013). Fingerprint quality assessment using a no-reference image quality metric. In *European Signal Processing Conference (EUSIPCO)*, page 6.
- Feng, J. and Jain, A. K. (2011). Fingerprint reconstruction: from minutiae to phase. *Pattern Analysis and Machine Intelligence, IEEE Transactions on*, 33(2):209–223.
- Grother, P. and Tabassi, E. (2007). Performance of biometric quality measures. *Pattern Analysis and Machine Intelligence, IEEE Transactions on*, 29(4):531–543.
- Hafiane, A., Seetharaman, G., and Zavidovique, B. (2007). Median binary pattern for textures classification. In *Image Analysis and Recognition*, pages 387–398. Springer.
- Hafiane, A. and Zavidovique, B. (2006). Local relational string for textures classification. In *Image Processing, 2006 IEEE International Conference on*, pages 2157–2160.
- Haralick, R. M., Shanmugam, K., and Dinstein, I. H. (1973). Textural features for image classification. *Systems, Man and Cybernetics, IEEE Transactions on*, (6):610–621.
- Jain, A. K., Ross, A., and Prabhakar, S. (2004). An introduction to biometric recognition. *Circuits and Systems for Video Technology, IEEE Transactions on*, 14(1):4–20.
- Lee, B., Moon, J., and Kim, H. (2005). A novel measure of fingerprint image quality using the Fourier spectrum. In Jain, A. K. and Ratha, N. K., editors, *Society of Photo-Optical Instrumentation Engineers (SPIE) Conference Series*, volume 5779 of *Society of Photo-Optical Instrumentation Engineers (SPIE) Conference Series*, pages 105–112.
- Lim, E., Jiang, X., and Yau, W. (2002). Fingerprint quality and validity analysis. In *Image Processing, 2002. Proceedings. 2002 International Conference on*, volume 1, pages 1–469–1–472 vol.1.
- Maio, D., Maltoni, D., Cappelli, R., Wayman, J. L., and Jain, A. K. (2004). Fvc2004: Third fingerprint verification competition. In *Biometric Authentication*, pages 1–7. Springer.
- Nanni, L. and Lumini, A. (2007). A hybrid wavelet-based fingerprint matcher. *Pattern Recognition*, 40(11):3146–3151.
- Nanni, L., Lumini, A., and Brahmam, S. (2012). Survey on lbp based texture descriptors for image classification. *Expert Systems with Applications*, 39(3):3634 – 3641.
- Ojala, T., Pietikainen, M., and Maenpaa, T. (2002). Multiresolution gray-scale and rotation invariant texture classification with local binary patterns. *Pattern Analysis and Machine Intelligence, IEEE Transactions on*, 24(7):971–987.
- Olsen, M. A., Xu, H., and Busch, C. (2012). Gabor filters as candidate quality measure for nfiq 2.0. In *Biometrics (ICB), 2012 5th IAPR International Conference on*, pages 158–163. IEEE.
- Pietikäinen, M. (2011). *Computer vision using local binary patterns*, volume 40. Springer.
- Ross, A. and Jain, A. (2004). Biometric sensor interoperability: A case study in fingerprints. In *Biometric Authentication*, pages 134–145. Springer.
- Ross, A., Shah, J., and Jain, A. K. (2005). Toward reconstructing fingerprints from minutiae points. In *Defense and Security*, pages 68–80. International Society for Optics and Photonics.
- Saad, M., Bovik, A. C., and Charrier, C. (2012). Blind image quality assessment: A natural scene statistics approach in the DCT domain. *IEEE Transactions on Image Processing*, 21(8):3339–3352.
- Shen, L., Kot, A., and Koo, W. (2001). Quality measures of fingerprint images. In *IN: PROC. AVBPA, SPRINGER LNCS-2091*, pages 266–271.
- Tabassi, E., Wilson, C., and Watson, C. (2004). Nist fingerprint image quality. *NIST Res. Rep. NISTIR7151*.
- Watson, C. I., Garris, M. D., Tabassi, E., Wilson, C. L., McCabe, R. M., Janet, S., and Ko, K. (2007). User's guide to nist biometric image software (nbis).
- YAO, Z., Charrier, C., and Rosenberger, C. (2014). Utility validation of a new fingerprint quality metric. In *International Biometric Performance Conference 2014*. National Insititure of Standard and Technology (NIST).

Table 5: Inter-class Pearson correlation for textural features. 02DB2A (top), 04DB1A (middle) and 04DB3A (bottom).

OCL	-0.6826	0.3002	-0.7037	-0.7895	-0.4462	-0.3294	0.3806	0.5864	0.6832	0.8699	-0.7593
OF	-0.1938	0.1783	0.0098	-0.0396	-0.0452	-0.0700	0.1685	0.2016	0.1590	-0.0012	0.0593
PHC	-0.6926	0.2864	-0.6665	-0.8805	-0.3391	-0.1957	0.3552	0.6329	0.7507	0.8476	-0.7807
STD	-0.6230	0.3958	-0.5590	-0.8796	-0.3016	-0.3037	0.5620	0.8066	0.8940	0.7668	-0.7438
NFIQ	0.3919	0.1240	0.3483	0.4675	0.1617	-0.0057	0.0401	-0.0676	-0.1307	-0.4569	0.2731
OCL	-0.6899	-0.7979	-0.7798	0.2582	0.7151	0.0456	0.4071	0.6708	0.7223	-0.7416	0.7125
OF	-0.2642	-0.3263	-0.3057	0.1580	0.2073	0.1087	0.3968	0.4206	0.4539	-0.2281	0.2057
PHC	-0.7060	-0.8206	-0.8416	0.2832	0.7535	0.0373	0.4722	0.7548	0.7964	-0.7701	0.7426
STD	-0.5920	-0.7066	-0.7286	0.2249	0.6471	0.0554	0.4669	0.6930	0.7264	-0.6646	0.6297
NFIQ	0.1634	0.1607	0.1775	-0.0683	-0.2101	-0.0412	0.0897	-0.0254	-0.0157	0.2295	-0.2143
OCL	-0.5001	-0.6394	-0.7460	0.0406	0.5144	0.0842	0.5301	0.6505	0.6948	-0.3814	0.5536
OF	-0.2510	-0.1842	-0.1539	0.1097	0.0814	-0.2304	-0.1348	-0.1148	-0.0539	-0.1537	0.1566
PHC	-0.1648	-0.2758	-0.4495	0.1015	0.1439	0.1660	0.6947	0.7992	0.7450	-0.1928	0.1726
STD	-0.2401	-0.3447	-0.5029	0.0839	0.2221	0.1201	0.6398	0.7359	0.7037	-0.2161	0.2550
NFIQ	-0.0532	-0.0886	0.0316	0.0183	0.0518	-0.2360	-0.3640	-0.4005	-0.2608	-0.0805	0.0907

Table 6: Inter-class Pearson correlation for image-based features. 02DB2A (top), 04DB1A (middle) and 04DB3A (bottom).

OCL	0.4816	0.2370	0.2931	0.1775	0.3659	-0.9137	0.6643	-0.8818	0.4179	-0.5538	-0.8443
OF	0.0386	-0.0438	0.1038	0.0733	0.2487	0.0391	0.0875	-0.0197	0.0840	-0.1092	0.0452
PHCWT	0.4720	0.3650	0.3149	0.1234	0.4921	-0.7480	0.5860	-0.7129	0.4031	-0.5316	-0.8469
STD	0.3169	0.2133	0.4788	0.2037	0.5805	-0.7170	0.6608	-0.6660	0.4149	-0.5252	-0.8023
NFIQ	0.4434	0.4445	0.1735	0.0971	0.1164	0.4017	0.2510	0.4088	0.1409	0.2598	0.3907
OCL	0.4689	0.0418	0.3839	0.4307	0.5980	-0.9129	0.8823	N	0.2666	-0.3423	0.8753
OF	0.1908	0.0065	0.1216	0.0284	0.1347	-0.1971	0.1586	NaN	-0.1877	0.2351	0.3396
PHC	0.5126	0.2468	0.4225	0.3492	0.7118	-0.7046	0.6858	N	0.2085	-0.2800	0.8687
STD	0.4070	0.2177	0.4946	0.3752	0.8112	-0.6632	0.6887	N	0.1722	-0.2416	0.7591
NFIQ	-0.1890	-0.3808	0.1444	0.0117	-0.3420	0.0132	-0.0121	N	0.0175	0.0069	-0.0719
OCL	0.3414	0.2499	0.2271	-0.0788	0.6927	-0.2067	0.6544	-0.5836	0.0446	-0.0068	0.7988
OF	-0.0558	-0.0645	-0.1039	-0.0052	0.0883	-0.0079	-0.1368	0.0741	-0.0361	-0.0017	0.0122
PHC	0.3580	0.4141	0.5300	-0.1290	0.5679	0.2351	0.8933	-0.2086	0.0303	0.0515	0.6215
STD	0.4175	0.4266	0.4661	-0.1211	0.6575	0.1858	0.9157	-0.2545	0.0262	0.0575	0.6319
NFIQ	-0.2256	-0.3925	-0.1761	0.2087	-0.2670	-0.2824	-0.4156	-0.0671	0.0335	0.0112	-0.1193

Table 7: Inter-class Pearson correlation for minutiae-based features. 02DB2A (top), 04DB1A (middle) and 04DB3A (bottom).

OCL	0.4077	0.3768	0.4040	0.2780	0.0826	0.3166	0.4214	-0.3196	-0.2799	-0.1930	-0.2568
OF	0.0327	0.0391	0.0442	-0.0096	0.0019	-0.0035	0.0491	-0.0040	-0.0987	0.0874	-0.0521
PHC	0.3717	0.3445	0.3735	0.2306	0.0298	0.2787	0.3829	-0.3230	-0.2704	-0.1934	-0.2791
STD	0.2391	0.2267	0.2376	0.1247	-0.0615	0.1630	0.2490	-0.2389	-0.2027	-0.1304	-0.1832
NFIQ	-0.6052	-0.5393	-0.5949	-0.4783	-0.4639	-0.5807	-0.5554	0.4461	0.3544	0.2975	0.3198
OCL	0.5576	0.5290	0.5570	0.4649	0.5088	0.4505	0.5536	-0.3599	-0.3677	-0.3178	-0.3986
OF	0.0835	0.0946	0.0859	0.1661	0.0721	0.1334	0.0128	0.0159	0.1975	-0.1621	-0.0372
PHC	0.4036	0.4153	0.4150	0.3462	0.3731	0.3124	0.4184	-0.2908	-0.3245	-0.2718	-0.3121
STD	0.3876	0.4017	0.4003	0.3275	0.3446	0.3149	0.3865	-0.2992	-0.3093	-0.2611	-0.3095
NFIQ	-0.1532	-0.1840	-0.1796	-0.1175	-0.1457	-0.1058	-0.1603	0.1778	0.1040	0.1771	0.1825
OCL	0.2447	0.2362	0.2521	0.1304	-0.0361	0.2280	0.2630	-0.2231	-0.1557	-0.1659	-0.2140
OF	0.2929	0.2577	0.2724	0.2786	0.3218	0.3043	0.2854	-0.0661	0.1458	-0.0830	-0.1077
PHC	-0.1438	-0.1170	-0.1215	-0.1919	-0.3633	-0.1563	-0.1144	-0.1132	0.0373	0.0158	0.0406
STD	-0.0421	-0.0243	-0.0220	-0.1007	-0.2618	-0.0561	-0.0130	-0.1491	-0.0271	-0.0423	-0.0281
NFIQ	0.3195	0.2497	0.2741	0.3971	0.4406	0.3391	0.2953	-0.0524	-0.0716	-0.0840	-0.0885